UCLA
UCLA Previously Published Works

Title
Broadband metasurface design for terahertz quantum-cascade VECSEL

Permalink
https://escholarship.org/uc/item/0w18c6zs

Journal
Electronics Letters, 56(23)

ISSN
0013-5194

Authors
Curwen, CA
Reno, JL
Williams, BS

Publication Date
2020-11-01

DOI
10.1049/el.2020.1963

Peer reviewed

Broadband metasurface design for terahertz quantum-cascade VECSEL

C. A. Curwen, J. L. Reno and B. S. Williams

A broadband active metasurface is designed around quantum-cascade (QC) gain material for use in a broadband tunable QC vertical-external-cavity surface-emitting laser (VECSEL). The metasurface is based on a unit cell containing two resonant waveguide elements that couple with the periodicity of the metasurface to produce a multi-resonant reflection spectrum. Simulated reflectance spectra exhibit full-width half-maximum bandwidths up to 50% of the centre frequency. The tested QC-VECSEL demonstrates up to 15 mW of peak pulse power at 77 K and supports multi-mode lasing from 2.85-3.9 THz (>30% fractional bandwidth around 3.37 THz). The frequency coverage is limited by how short the cavity can be made, rather than the metasurface bandwidth. Consistent multi-moding results from a non-uniform distribution of spectral energy across the surface.

Introduction: Metasurfaces loaded with III-V heterostructure quantum wells that support intersubband transitions have been demonstrated as improved sources and detectors in the mid-IR [1] and THz frequency ranges [2, 3]. One such example is the THz quantum-cascade (QC) vertical-external-cavity surface-emitting-laser (VECSEL). The inclusion of THz QC-gain material produces an amplifying reflector that can be used to build an external cavity laser [4]. Thanks to the combination of a broadband response from the metasurface and the ability to tune the external cavity length, the QC-VECSEL lasing frequency can be tuned over a broad range – on the order of 20% fractional tuning around the centre frequency [5]. However, THz QC active material has demonstrated octave-spanning bandwidths (66% fractional [6]), so it is desirable to have similarly broadband metasurfaces with which to pair. In this study, we present a modified QC metasurface based upon a coupled-resonator approach that allows significant increases of the amplification bandwidth.

Single-ridge metasurface: The typical metasurface design used with the THz QC-VECSEL consists of an array of narrow (~10-15 μm wide) metal-metal ridge waveguides loaded with THz QC-gain material [7]. Each ridge supports a transverse resonance which is primarily determined by the width of the ridges according to the relation $w \approx \lambda_0/2n$, where λ_0 is the free space wavelength at the centre of the ridge resonance, and n is the refractive index of the QC-material. This resonance is strongly coupled to surface normal radiation, much in the same manner as an elongated microstrip patch antenna. The periodicity of the ridges is kept subwavelength to prevent diffraction effects at normal incidence. This resonance is deliberately engineered to have a relatively low quality factor Q to ensure that when gain is applied it will not self-oscillate; rather the metasurface requires feedback from an external cavity to form a laser. The metasurface Q is dominated by radiative losses, and is strongly dependent on the period Λ. As Λ approaches λ_0, reduced radiative losses increase the quality factor. Conversely, reducing the period reduces Q, and broadens the spectral response of the metasurface. However, broadening the metasurface response in this way also results in reduced amplification (lower Q means the radiation spends less time in the metasurface) which necessitates higher reflectance output couplers and more stringent control of diffraction losses.

Double-ridge metasurface: In order to increase the bandwidth without excessively reducing the amplification, we consider now a coupled-resonator metasurface design with two ridge elements per period, whose widths and separation can be varied. To understand such a scenario, consider the metasurface in Fig. 1, which is targeted to operate between 3-4 THz. It consists of two ridges that have equal widths and are equally spaced. Technically, this is no different than a single ridge metasurface with a period of $\Lambda/2$, and the reflectance spectrum shows a single, broad, low reflectance resonance, as expected. Eigenfrequency simulations reveal three resonances (Fig. 1(b)). At ω_1 is the conventional "patch" antenna resonance with a very low quality factor; at ω_2 and ω_3 are two Bragg modes with opposite modal symmetry and

fields localized in the semiconductor and vacuum respectively. As long as the ridges are equally sized and spaced, these modes are dark and do not influence the reflection spectrum of the metasurface. If, however, the symmetry is broken by making the ridges different widths, the resonance at 3.48 THz becomes bright and appears in the reflection spectrum. If the symmetry is broken by spacing the ridges differently, the Bragg mode at 4.28 THz becomes bright. Small perturbations add small radiative loss and result in high quality factor resonances, while larger perturbations broaden them. The green curve was generated by reducing the spacing between the two ridges by 10%, and the purple curve was generated by making one ridge 3% wider than the other. We note that this structure is essentially identical to the 2nd order distributed feedback cavity that is presented in Ref [8], but operates in a different regime of the parameter space where the radiative loss is much stronger and the localized solution is closer to the Bragg modes. In this sense, the structure blurs the lines between a grating coupler and a meta-structure.

With this conceptual model, we present simulated reflectance spectra of several exemplar designs in Fig. 2. The solid and dashed black curves indicates the reflectance of a single ridge surface with a period of $\Lambda = 20.9$ μm (same as Fig. 1) and $\Lambda = 70$ μm respectively. The red curve indicates an optimized design with two ridges of different widths but evenly spaced (this is the device that was fabricated and tested). The blue curve shows an optimized design where both the ridge width and spacing are varied. While all of the curves exhibit broad bandwidth, the asymmetric surfaces provide higher reflectance as they effectively combine several higher quality factor resonances rather than using a single low quality resonance. The full-width half-maximum (FWHM) bandwidth is increased from ~20% fractional for the single-ridge metasurface, to ~50% fractional for the blue curve with similar reflectance values.

As dispersion is often a concern in broadband applications, the group delay dispersion (GDD) of the metasurfaces (neglecting intersubband and material contributions) is simulated and plotted in the upper portion of Fig. 2. It is observed that all of the double ridge designs show spectral regions that are hundreds of gigahertz wide while maintaining a low GDD. The red curve (fabricated design), for example, keeps GDD within ± 0.1 ps^2 over a range of 750 GHz, comparable to the GDD associated with many THz QCL frequency comb devices [9-11].
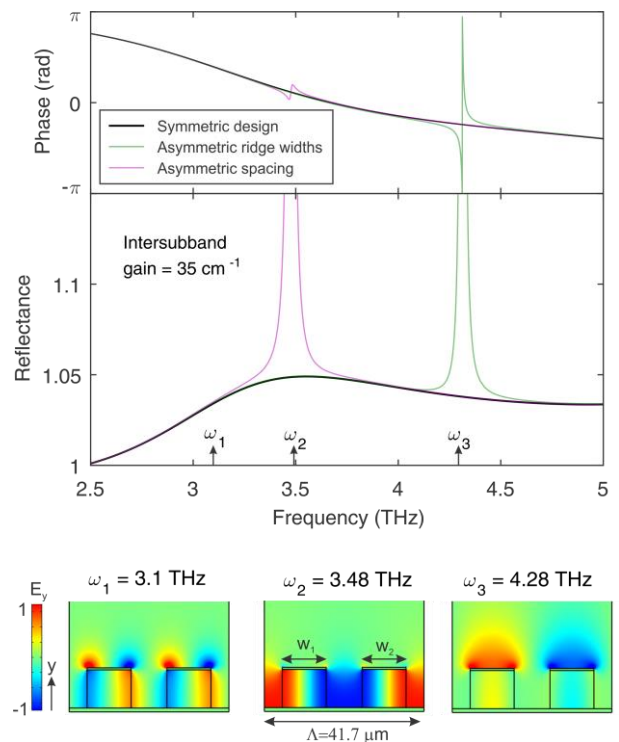

Fig. 1 *Double-ridge metasurface with equal and nearly equal ridge widths and spacings*
a Reflection magnitude and phase.
*b* Eigenfrequency electric-field plots.
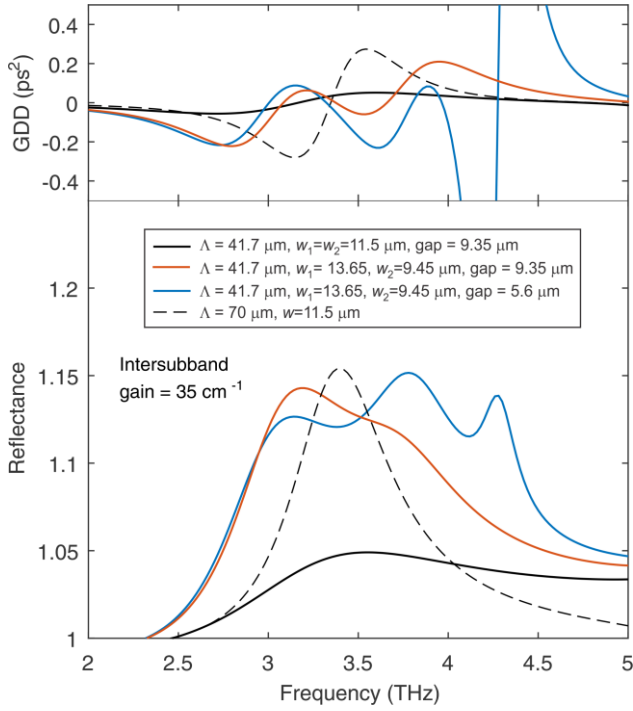
Fig. 2 *Reflectance and group delay dispersion of several amplifying metasurface designs.*

Experimental results: To study the double-ridge metasurface, we have fabricated and tested the metasurface design represented by the red curve in Fig. 2 (different ridge widths, but equal spacing). The active material used was a high-performance hybrid resonant-phonon design, also used in Ref. [5] (wafer VB0739), which is known to exhibit a broad gain-bandwidth. The metasurface is 2×2 mm^2 in area where electrical bias is applied only to a circular central area of 0.75 mm diameter. The lasing frequency of the VECSEL is determined by the round trip condition $2kL_{EC} - \varphi_{meta} - \varphi_{OC} = 2\pi m$, where $k = 2\pi f/c$ is the free space wavenumber of the lasing frequency, L_{EC} is the length of the external cavity, and φ_{meta} and φ_{OC} are the frequency dependent reflection phases of the metasurface and output coupler respectively. Therefore, we can tune the lasing frequency by simply changing the length of the external cavity (see Ref [5]). To adjust the length of the cavity, we use piezoelectric stack actuators (Noliac NAC2121-H28 which provide 43 μm actuation range at room temperature). The output coupler mirror (described in Ref. [7]) exhibits reflectance greater than 97% over the entire metasurface bandwidth. The high reflectance of the output coupler is used to maximize the potential bandwidth of lasing that can be observed by minimizing threshold gain values.
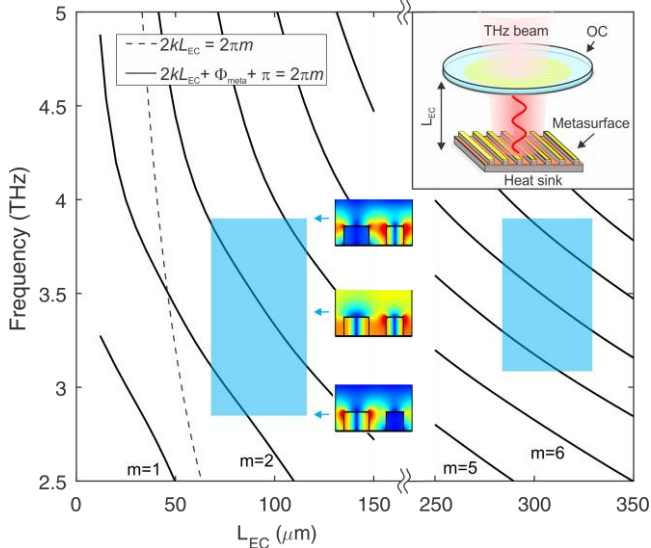
Fig. 3 *QC-VECSEL cavity setup and resonant solutions as a function of cavity length. Blue shaded regions correspond to data in Fig. 4.*
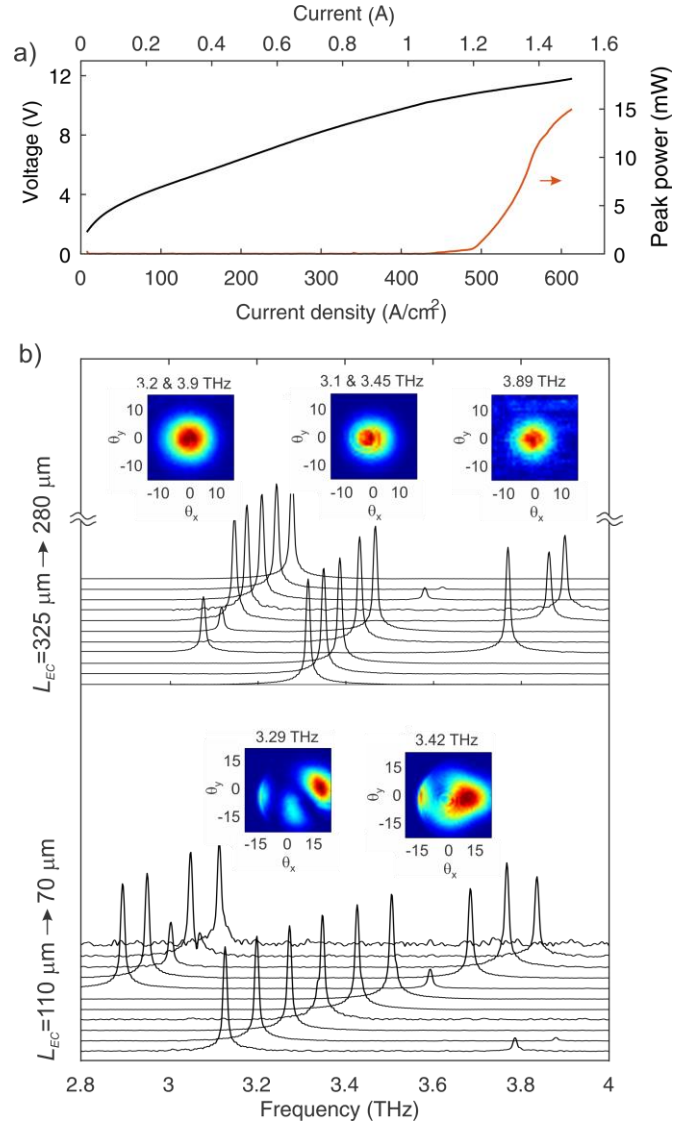
Fig. 4 *Experimentally measured QC-VECSEL characteristics.*
a Power and voltage vs. current characteristic at 3.44 THz.
b Spectra and beam patterns measured while tuning cavity length.

In order to observe lasing over the largest range possible, the length of the external cavity L_{EC} was kept short so as to maximize the free spectral range (FSR) between cavity modes and force the VECSEL to lase on the outer wings of the metasurface response. This effect is illustrated in Fig. 3, where the external cavity mode frequencies are plotted as a function of the cavity length. Although the metasurface phase has the effect of reducing the spacing between modes that would be present in a simple Fabry-Perot resonator ($\Delta f = c/2L_{EC}$), there is still expected to be upwards of 600 GHz of tuning of a given mode at the shortest cavity lengths.

The device was tested at 77 K in pulsed mode with a 10 kHz repetition rate and 1 μs pulse widths. A sample power-current-voltage (*P-I-V*) curve is shown in Fig. 4. Relative output power was measured using a pyroelectric detector (GentecEO), and absolute power was measured with a calorimeter (Scientech). Approximately 15 mW of peak power was observed at 3.44 THz, where the largest signal was observed, but the power varies with frequency in response to the varying metasurface response, intersubband gain, and output coupler reflectance. The normalized spectra collected as the cavity length is tuned is plotted in Fig. 4. Between one and three modes are observed to lase simultaneously as the cavity is tuned as a result of some detailed mode competition that is not well understood. While we are not able to directly measure the length of the external cavity, because of the multi-moding, the cavity length can be estimated from the simulation in Fig. 3 to vary from 325-280 μm in the upper portion of Fig. 4 (3.07-3.91 THz), and 115-70 μm in the bottom portion of the figure (2.85-3.9 THz). A collection of beam patterns measured throughout the tuning range are

plotted. At the longer cavity lengths, generally circular beam patterns are observed with a divergence angle of ~10°, but at the shorter cavity lengths, the beam breaks into multiple lobes (some of the beam cut-off by the edge of the cryostat window). This behaviour could possibly be the result of complicated near field solutions occurring when the output coupler is within a wavelength or so of the metasurface (discussed briefly in reference [5]), possibly exacerbated by cavity misalignment of the output coupler with the metasurface.

Conclusions: We have shown that using two inhomogeneous resonators per unit cell is a viable path towards increasing the amplification bandwidth of QC metasurfaces. Multi-mode lasing is demonstrated over a range of frequencies spanning 31% fractional bandwidth around a centre lasing frequency of 3.37 THz. However the measured range in this device is likely limited by the gain bandwidth of the underlying active material and the cavity itself rather than the metasurface bandwidth. Simulations predict larger bandwidths are possible, which may be well suited to use with octave-spanning heterogeneous QC active region designs [6]. While the gain bandwidth was too great to sustain single mode tuning in a short-cavity configuration, use of intracavity frequency filtering elements such as gratings or etalons may allow single-mode operation. This metasurface design may also be useful for broadband multi-mode sources (e.g. frequency combs or low coherence sources), particularly since the metasurface group delay dispersion is reduced compared with a single ridge design. The presence of three lasing modes is noteworthy in and of itself, since in previous QC-VECSEL demonstrations based upon single-resonator metasurfaces, at most double-mode lasing has been observed, despite operating at cavity lengths where the FSR is small compared the gain bandwidth of the QC/metasurface system [7]. We speculate that this is because spatial hole burning manifests differently than in a conventional waveguide-based QCL. In a single-ridge metasurface VECSEL all longitudinal cavity modes are coupled to the to the QC active material via the same half-wavelength resonance; hence all modes compete for gain within the same active region volume. The coupled resonator metasurface, on the other hand, is expected to exhibit an increased degree of spatial hole-burning in that different portions of the spectral profile are localized in different portions of the metasurface (see Fig. 3). Such an interpretation is further bolstered by the spectra in Fig. 4, in which it appears that the QC-VECSEL prefers to lase either multi-mode at one high and one low frequency (each mode extracting gain mostly from one of the coupled ridges), or to lase single-mode on a centrally located frequency (which draws gain from both ridges). The issue is particularly relevant for broadband QC-VECSELs, since spatial hole burning is believed to be a important element in driving the formation of THz QCL frequency combs [12]. Future research should investigate whether a higher degree of multimoding can be sustained within a QC-VECSEL, the external cavity must be made longer considerably longer to reduce the FSR – in this initial demonstration large diffraction losses associated with the implemented plano-plano cavity and small bias area prevented operating with cavities longer than ~1 mm. Another promising avenue will be metasurfaces with increased inhomogeneity deliberately introduced to promote multi-moding.

Christopher A. Curwen, Benjamin S. Williams (*Department of Electrical and Computer Engineering, University of California, Los Angeles, California 90095, USA*).

E-mail: ccurwen@ucla.edu

John L. Reno (*Sandia National Laboratories, Center of Integrated Nanotechnologies, MS 1303, Albuquerque, New Mexico 87185, USA*)

References:

1. D. Palaferri, Y. Todorov, A. Bigioli, *et al.*, "Room-temperature nine-μm-wavelength photodetectors and GHz-frequency heterodyne receivers," *Nature,* 2018, vol. 556, pp. 85-88.
2. D. Palaferri, Y. Todorov, Y. N. Chen, *et al.*, "Patch antenna terahertz photodetectors," *Appl. Phys. Lett.,* 2015, vol. 106, (16).
3. J. Perez-Urquizo, J. Madeo, Y. Todorov, *et al.*, "Patch Antenna Microcavities THz Quantum Cascade Lasers," *2019 44th International Conference on Infrared, Millimeter, and Terahertz Waves (IRMMW-THz),* 2019.
4. L. Y. Xu, C. A. Curwen, P. W. C. Hon, *et al.*, "Metasurface external cavity laser," *Appl. Phys. Lett.,* 2015, vol. 107, (22).
5. C. A. Curwen, J. L. Reno, and B. S. Williams, "Broadband continuous single-mode tuning of a short-cavity quantum-cascade VECSEL," *Nat. Photon.,* 2019, vol. 13, (12), pp. 855-859.
6. M. Rosch, G. Scalari, M. Beck, *et al.*, "Octave-spanning semiconductor laser," *Nat. Photon.,* 2015, vol. 9, (1), pp. 42-47.
7. L. Y. Xu, C. A. Curwen, D. G. Chen, *et al.*, "Terahertz metasurface quantum-cascade VECSELs: theory and performance," *IEEE J. Sel. Top. Quantum Electron.,* 2017, vol. 23, (6).
8. L. Mahler, A. Tredicucci, F. Beltram, *et al.*, "High-power surface emission from terahertz distributed feedback lasers with a dual-slit unit cell," *Appl. Phys. Lett.,* 2010, vol. 96, (19).
9. D. Burghoff, Y. Yang, J. L. Reno, *et al.*, "Dispersion dynamics of quantum cascade lasers," *Optica,* 2016, vol. 3, (12), pp. 1362-1365.
10. D. Bachmann, M. Rosch, G. Scalari, *et al.*, "Dispersion in a broadband terahertz quantum cascade laser," *Appl. Phys. Lett.,* 2016, vol. 109, (22).
11. F. P. Mezzapesa, V. Pistore, K. Garrasi, *et al.*, "Tunable and compact dispersion compensation of broadband THz quantum cascade laser frequency combs," *Opt. Express,* 2019, vol. 27, (15), pp. 20231-20240.
12. N. Henry, D. Burghoff, Q. Hu, *et al.*, "Temporal characteristics of quantum cascade laser frequency modulated combs in long wave infrared and THz regions," *Opt. Express,* 2018, vol. 26, (11), pp. 14201-14212.